



HAL
open science

Optimizing the physical properties of collagen/hyaluronan hydrogels by inhibition of polyionic complexes formation at pH close to the collagen isoelectric point

Stéphanie de Oliveira, Gregor Miklosic, Joëlle Veziers, Sébastien Grastilleur,
Thibaud Coradin, Catherine Le Visage, Jérôme Guicheux, Matteo D'este,
Christophe Hélyary

► To cite this version:

Stéphanie de Oliveira, Gregor Miklosic, Joëlle Veziers, Sébastien Grastilleur, Thibaud Coradin, et al.. Optimizing the physical properties of collagen/hyaluronan hydrogels by inhibition of polyionic complexes formation at pH close to the collagen isoelectric point. *Soft Matter*, 2023, 19 (46), pp.9027-9035. <10.1039/d3sm01330h>. <hal-04299962>

HAL Id: hal-04299962

<https://hal.science/hal-04299962v1>

Submitted on 22 Nov 2023

HAL is a multi-disciplinary open access archive for the deposit and dissemination of scientific research documents, whether they are published or not. The documents may come from teaching and research institutions in France or abroad, or from public or private research centers.

L'archive ouverte pluridisciplinaire HAL, est destinée au dépôt et à la diffusion de documents scientifiques de niveau recherche, publiés ou non, émanant des établissements d'enseignement et de recherche français ou étrangers, des laboratoires publics ou privés.



HAL Authorization

**Optimizing the physical properties of collagen/hyaluronan
hydrogels by inhibition of polyionic complexes formation at pH
close to the collagen isoelectric point**

Stéphanie De Oliveira ^a, Gregor Miklosic ^b, Joëlle Veziers ^c, Sébastien Grastilleur^c,
Thibaud Coradin ^a, Catherine Le Visage ^c, Jérôme Guicheux ^c, Matteo D'Este ^b,
Christophe Hélyary ^{a*}

^a Sorbonne University - Laboratory of Condensed Matter Chemistry of Paris, CNRS, UMR
7574
Campus Pierre et Marie Curie, 4 place Jussieu, 75252 Paris Cedex 05, France

^b AO Research Institute Davos (ARI), Clavadelerstrasse 8, 7270 Davos, Switzerland

^c Nantes Université, Oniris, INSERM, Regenerative Medicine and Skeleton, RMeS, UMR 1229,
Faculté d'Odontologie 1 place Alexis Ricordeau 44000 NANTES;

* Corresponding authors: Christophe Hélyary

Email address: christophe.helary@sorbonne-universite.fr

Telephone: +33144276539

Abstract

Collagen/hyaluronan hydrogels with physical properties well suited for biomedical applications are challenging to synthesize due to the formation of polyionic complexes (PICs). A systematic physicochemical study was thus performed to determine novel conditions to inhibit the formation of collagen/hyaluronan PICs and obtain composite hydrogels with high physical properties. Using a range of pH from 1 to 5.5 and the addition of NaCl, type I collagen and tyramine-substituted hyaluronic acid (THA) solutions were mixed and analyzed by cryo-scanning electron microscopy and ATR-FTIR. PIC formation was inhibited at pH 1 without salt and at pH 2.5 and 5.5 in the presence of 400 mM NaCl. Interestingly, collagen fibrils were observed in solution at pH 5.5 before mixing with THA. After collagen gelling by pH increase, a homogeneous hydrogel consisting of collagen fibrils was only observed when PICs were inhibited. Then, the THA gelling performed by photo-crosslinking increased the rheological properties by four when hydrogels were formed with collagen/THA mixtures at pH 1 or 5.5 with salt. Taken together, these results show that a pH of 5.5, close to the collagen isoelectric point, enables the formation of collagen fibrils in solution, inhibits the PICs formation, and allows the formation of homogenous collagen/THA composite hydrogels compatible with cell survival.

Keywords

Collagen, hyaluronic acid, polyionic complexes, hydrogels, photocrosslinking, isoelectric point.

1. Introduction

Hydrogels are promising materials for tissue engineering applications as they are highly hydrated with tunable mechanical properties. In addition, they allow for the rapid diffusion of nutrients and oxygen through the scaffold¹. Last, mechanical irritation on the surrounding tissues after implantation is low². They can be synthesized from natural or synthetic polymers that form physically or chemically crosslinked networks³.

Biopolymers are of great interest in tissue engineering through their biocompatibility and ability to mimic the natural cellular environment^{4,5}. Type I collagen is the main component of mammalian extracellular matrices and is at the origin of the fibrous structure and resistance of tissues. This protein is broadly used for biomedical applications as it is the natural support for cells⁶. Collagen-based hydrogels are usually fabricated from low-concentrated (less than 5 mg/mL) solutions by pH increase, up to 7 to form a physical hydrogel composed of collagen fibrils⁷. The main limitation of these biomaterials is their low stability in vivo, mainly due to their fast degradation. In addition, the collagen network contracts under the cellular activities of fibroblasts or stem cells^{8,9}.

Hyaluronic acid is a non-sulfated glycosaminoglycan naturally present in the extracellular matrix. Due to its biological properties, water retention properties, and capability to be chemically modified to modulate its properties, hyaluronan is broadly used in tissue engineering and 3D printing. In its native form, this polysaccharide does not form hydrogels⁸. To fabricate hyaluronan-based hydrogels, it is necessary to functionalize the polysaccharide chain with a cross-linkable function such as Tyramine. Tyramine-substituted hyaluronan (THA) gelation can be performed using several methods including enzymatic (Horseradish Peroxidase/H₂O₂) or photocrosslinking. The Horse Radish Peroxidase (HRP) / H₂O₂ system is

an interesting candidate to control the crosslinking density and gelation kinetic. In addition, the mild conditions do not produce cytotoxic by-products^{2,9,10}. Photocrosslinking relies on the use of photoinitiators which produce reactive species upon light exposure. Visible light is recognized to enable higher cell survival than UVs¹¹. Eosin Y used as photoinitiator can be exposed to green light to efficiently gel THA. At an optimized concentration and exposure time, it is not cytotoxic for cells and allows fast gelation into covalent networks with tunable properties¹⁰. The latter depends on molecular weight and degree of substitution by tyramine moieties. However, cell adhesion to THA hydrogels is low and it is therefore often combined with another biopolymer allowing for cell survival^{12,13}.

Collagen/hyaluronic acid composite hydrogels have been broadly studied to develop biomaterials used in tissue engineering. Combining intrinsic properties of both biopolymers is interesting for biomedical applications such as dermal filling, intervertebral disc regeneration, cartilage and bone repair. Due to a strong interaction between positively-charged collagen and negatively-charged hyaluronic acid, polyionic complexes (PICs) readily form in solution¹³. These biopolymers tend to precipitate and are therefore difficult to use to generate composite hydrogels. To circumvent this issue, one strategy is to form one hydrogel first and then add the second biopolymer¹⁴. However, such an association is not always beneficial to the properties of the composite hydrogel¹⁵. Collagen fibrillogenesis can be altered within HA hydrogels and HA incorporation into collagen hydrogels can modify mechanical properties¹⁶. Another strategy is to form a hybrid network following the chemical functionalization of both collagen and HA. In this case, collagen fibrillogenesis is completely inhibited. Without fibrillar structure, these materials do not reproduce the natural topography of extracellular matrices. Last, both polymers can be pre-neutralized before mixing¹⁵. At pH 7, collagen is close to neutral, thereby limiting electrostatic interactions with HA. However, the pH increase triggers

a fast collagen gelling. Hence, collagen/THA solutions have to be immediately used after mixing. As a consequence, composite materials cannot be produced by 3D printing, electrospinning or spray drying that require an initial solution stable over the whole processing duration, i.e. tens of minutes^{17,18}. A few studies investigated how to inhibit PICs formation in solution. Chen et al have shown that the PICs formation could be inhibited by the addition of NaCl in highly acidic conditions (pH 1)¹⁷. Nevertheless, no studies on hydrogels formation from these acidic solutions have been conducted. Only crosslinked sponges synthesized by freeze drying of acidic collagen/HA solutions have been described. In addition, no systematic studies on the impact of pH and the presence of salt have been performed either.

In this study, we investigated polyionic complexation between collagen and tyramine functionalized hyaluronic acid in order to identify novel conditions for its inhibition. This would allow to generate homogeneous collagen/THA hydrogels with physical properties suitable for biomedical application (structure and mechanical properties). For this purpose, a range of pH was tested in collagen/THA mixtures followed by salt addition to evaluate the physicochemical behavior of these biopolymers in solution. Then, hydrogels were formed by triggering first the collagen gelling using pH increase. Then, THA gelling was carried out using the enzymatic or photo-crosslinking. Last, the physical properties of the as-made collagen/THA composite hydrogels were analyzed in detail.

2. Materials and methods

2.1. Materials

Hyaluronan sodium salt from *Streptococcus equi* with weight average Molecular Weight (MW= 290 kDa) and dispersity index of 1.86 was purchased from Contipro Biotech s.r.o (Czech

Republic). 4-(4,6-Dimethoxy-1,3,5-triazin-2-yl)-4-methylmorpholinium chloride (DMTMM) was purchased from TCI Europe N.V. (Tokyo, Japan), Tyramine hydrochloride (Tyr), hydrogen peroxide, horseradish peroxidase, NaOH, NaCl and eosin Y were purchased from Merck (France). HCl (37 %), acetic acid (99-100 %), and absolute ethanol were purchased from VWR International (France). 1X PBS was obtained from Thermo Fischer Scientific.

2.2. Collagen extraction and purification

Native type I collagen was extracted from tails of Young Wistar male rats as previously described ¹⁹. Basically, rat tails were rinsed with 70% ethanol, placed in a safety cabinet and cut in 1 cm sections from their extremity to extract tendons. After several rinses in 1X PBS, tendons were solubilized in 500 mM acetic acid for 24 hours. Then, collagen was purified by precipitation using 0.7 M NaCl. Precipitates were dissolved in a fresh 500 mM acetic acid solution. Salt elimination was performed by dialysis against 500 mM acetic acid. The final solution was centrifuged for 4 hours at 30000 g to remove aggregates and supernatant was stored at 4 °C. The collagen concentration was determined by hydroxyproline titration ²⁰ and purity assessed by SDS-PAGE electrophoresis (MiniProtean TGX, Biorad). Finally, the concentration was set to 6 mg.mL⁻¹ via evaporation under a safety cabinet. Dialysis of the collagen solution was performed against different HCl solutions with concentration from 10⁻¹ to 10⁻⁵ M to set the pH value from 1 to 5.5.

2.3. Hyaluronic acid functionalization with Tyramine

Hyaluronan functionalization was conducted by amidation reaction of the carboxylic acid moieties from HA and the amine group from Tyramine hydrochloride using DMTMM as previously described ²¹. For this purpose, hyaluronic acid sodium salt (2g, 5mmol carboxylic

groups) was dissolved overnight in 200mL of ultrapure water at a final concentration of 1 % (w/v). HA solution was then warmed up to 37°C using a thermostatic oil bath. 1,38 g of DMTMM was added to the HA solution and then a cap was set to keep the system closed. In parallel, Tyramine hydrochloride (5 mmol) was dissolved in 5 mL of MilliQ water and then added dropwise to the mixture. The reaction was conducted at 37 °C under stirring for 24 h. The following day, 32 mL of a saturated NaCl solution was added and stirred for 30 minutes. The tyramine-modified Hyaluronan (THA) precipitation was then performed by adding dropwise 96 % alcohol (600 mL). The precipitate was collected by filtration under vacuum using a Gooch filter P3. After several washes with 80% ethanol (500 mL), 90% ethanol (200 mL), 96 % ethanol (200 mL) and absolute ethanol (200 mL), the solid was spread on a glass petri dish, left in the hood overnight and finally dried at 40 °C for 48h. Salt residues were detected with a silver nitrate (0.1 M) and molar degree of substitution was determined using by measuring absorbance at 275 nm of 0,1 % (w/v) THA solution in MilliQ water using a Cary 5000 UV-vis-NIR Spectrophotometer (Agilent Technologies). Standards with Tyramine hydrochloride were used to calculate THA degree of functionalization in a concentration range between 0 and 1000 µg/mL. THA was dissolved in different HCl solutions (10^{-1} to 10^{-5} M) to a final 30 mg.mL⁻¹.

2.4. Mixtures of Collagen and THA

The collagen solutions (6 mg.mL⁻¹) and the THA solutions (30 mg.mL⁻¹) prepared with HCl concentrations from 10^{-1} M to 10^{-5} M, with or without NaCl at 400 mM, were used for this experiment. The solutions were stirred for 24h at room temperature prior to their utilization. The following day, collagen (666 µL) and THA (133 µL) were mixed at a 1:1 mass ratio (w/w)

with a positive displacement micropipette (Gilson) to reach a $4 \text{ mg}\cdot\text{mL}^{-1}$ concentration for both biopolymers. Then, the mixtures were stirred for 12 h at room temperature.

2.5. Gelling and fibrillogenesis of collagen/THA solutions

Collagen fibrillogenesis and gelling of collagen/THA mixtures was triggered by pH increase. To do so, 200 μL of previously prepared mixture was poured into small molds (7 mm in diameter) and placed under ammonia vapors for 24 h. The day after, resulting hydrogels, 5 mm thick, were extensively washed with MilliQ water until a neutral pH was reached.

2.6. THA crosslinking within Collagen/THA hydrogels.

After collagen gelling, THA crosslinking was performed using two different methods to obtain interpenetrated network hydrogels. (i) Enzymatic crosslinking was carried out using Horse Radish Peroxidase (HRP) and Hydrogen Peroxide (H_2O_2). 100 μL of HRP/ H_2O_2 solution, ([HRP] = $1.5 \text{ UI}\cdot\text{mL}^{-1}$, [H_2O_2] = 1.1 mM) was added on top of collagen/THA hydrogels. Hydrogels were then incubated at room temperature on a stirring plate covered with a tin foil for 24 hours to allow chemical crosslinking (formation of di-tyramine bonds.) The second method was based on photocrosslinking using an eosin Y / green LED light system. Eosin Y was firstly solubilized in DMSO to generate a stock solution concentrated at $200 \text{ mg}\cdot\text{mL}^{-1}$ and then diluted in water to reach a final concentration at $200 \mu\text{g}\cdot\text{mL}^{-1}$. Collagen/THA hydrogels were immersed in an Eosin Y bath (2 mL) overnight in a 24 well plate protected from the light. The Eosin homogeneity was checked by observation of its orange color throughout hydrogels. The following day, hydrogels were removed from the eosin bath and photocrosslinked under green LED light for 90 min (hydrogels placed at 10 cm from the led lamp). The green light could

be observed through hydrogels, thereby evidencing the effective crosslinking. Hydrogels were then washed extensively with MilliQ water until the orange color due to the eosin presence disappeared.

2.7. Cryogenic Scanning Electron Microscopy (Cryo-SEM) analysis

Collagen/THA mixtures were processed for cryo-SEM using the PP3010T, QUORUM cryo preparation system (Laughton, United Kingdom). For this purpose, a drop of each collagen/THA mixture with or without NaCl was placed between two rivets. Then, rivets were set onto a sample holder attached to a shuttle. The freezing step was performed in slush nitrogen, cooled by pressure drop (9×10^{-2} mBar) to approximately -206 °C. After introduction into the preparation chamber, the samples were cryo-fractured, sublimated (4 min at -100 °C), and sputtered with palladium (50 s, 10 μ A).

The samples were then introduced into the electron microscope and positioned on the cold stage (-140 °C). Observations were performed on a Gemini SEM 300, ZEISS (Oberkochen, Germany) at 2 kV, 30 μ m diaphragm, using either SE2 detector positioned in the chamber or SE2 detector (Inlens) positioned in the column (n=3).

2.8. ATR-FTIR analysis

ATR-FTIR analyses were conducted on the different collagen/THA fibrillated hydrogels to identify possible interactions between collagen and THA when PICs are formed. To do so, composite hydrogels were freeze-dried for 24 h in 1 mL microfuge tubes. Dried hydrogels were cooled in ice and blended with a mortar. Then, they were analyzed using Attenuated Total Reflectance (ATR)-FTIR method using a Perkin Elmer Spectrum 100 equipment. Samples were

deposited on the diamond crystal and pressed to optimize signal intensity (n=3). For each spectrum, 64 scans were collected between 500 and 4000 cm^{-1} with a measure every 1 cm^{-2} . For each condition, three spectra were acquired and the mean was calculated for each sample.

2.9. Differential Scanning Calorimetry (DSC)

DSC was conducted on collagen/THA solutions or hydrogels to measure the denaturation temperature of collagen in different conditions. One mL of mixtures was freeze-dried for 24 hours and then rehydrated with 15 μL of the solvent used for their synthesis (*i.e* the appropriate NaCl and HCl concentrations). Regarding hydrogels, 1 mL of hydrogel was freeze-dried, and 20 μL of MilliQ water was used to rehydrate them after lyophilization. Then, 5 to 10 mg of rehydrated hydrogel or collagen/THA solution was placed within hermetically closed aluminium pans. Samples were analyzed using a modulated DSC TA Q20 (Texas Instrument). Standby temperature was set at 20°C, then increased from 10 °C to 90 °C at a heat speed of 10 °C.min⁻¹. Data were analyzed using TA Universal Analysis software (n=3). Denaturation temperatures were calculated using the mean of triplicates for each condition.

2.10. Rheological measurements

Shear oscillatory measurements were performed on collagen/THA hydrogels using an Anton Paar rheometer MCR302 fitted with a 7.5 mm sand-blasted parallel plate upper geometry. All tests were performed at 20 °C with sweep frequency (from 0.1 to 10 Hz). Mechanical spectra, namely storage G' and loss G'' moduli versus frequency, were recorded at an imposed 1% strain, which corresponds to non-destructive conditions, as previously checked with an amplitude sweep (data not shown). In order to test all hydrogels in the same conditions,

before each run, the gap between base and geometry was chosen to apply a 0.1 N positive normal force on gels during measurement. At least 3 hydrogels per condition were tested.

2.11. Scanning Electron Microscopy (SEM) analysis

Collagen hydrogels were imaged using SEM before and after THA crosslinking. Hydrogels were first fixed using a glutaraldehyde solution at 4% in PBS overnight, then washed three times in a cacodylate 0,1 M/saccharose 0,6 M buffer (1 vol/1 vol) and dehydrated using different ethanol baths with increasing concentration (from 50 % to 100 %). Last, samples were dried using a super critical dryer (Leica). Dried samples were then scratched, stuck onto holders and sputtered with a 15 nm gold layer (n=3). Observations were carried out with a Hitachi S-3400N SEM operating at 10 kV with a probe current around 95 μ A. Images were captured at a magnification of X 20k.

2.12. Statistical analysis

All experiments were carried out at least twice, and the results were expressed as mean values \pm standard deviation (SD). The differences between the different formulations were analyzed for each time point using Kruskal-Wallis test. Then, a Dunn Test was used as post-hoc test to determine the differences between groups. A p value < 0.05 was considered significant.

3. Results and discussion

3.1. Preparation and characterization of Collagen/ THA solutions

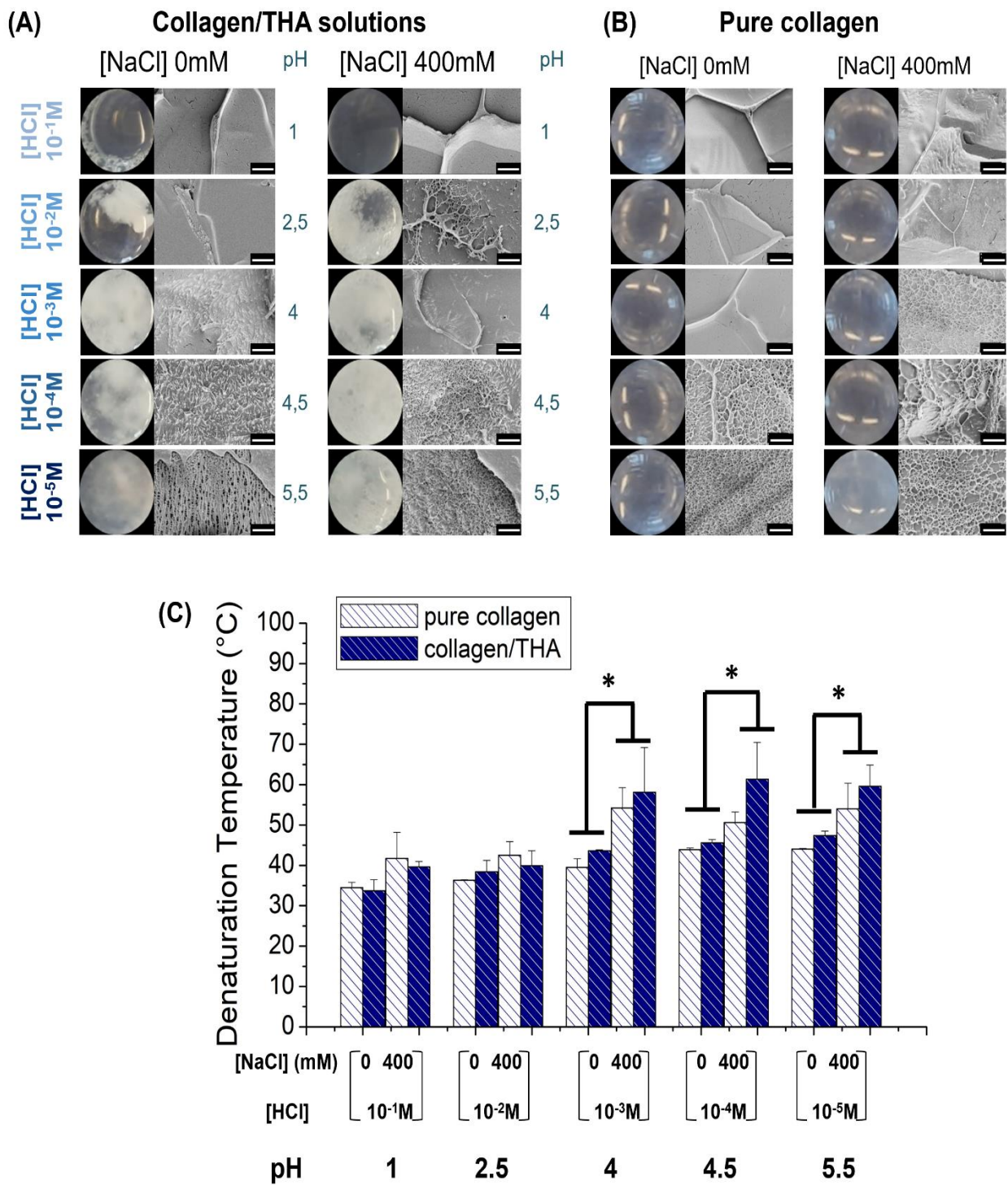


Figure 1 : (A) Collagen/THA solutions (0.4%/0.4% w/v) observed with CryoSEM (scale bar: 1 μ m) and their corresponding macroscopic views. (B) Pure collagen hydrogels observed with CryoSEM (Scale bar: 1 μ m). (C) Denaturation temperatures of collagen in the different formulations measured by Differential Scanning Calorimetry (DSC). *: $p < 0.05$ ($n=3$).

Mixing THA and collagen at pH 1 generated clear and homogenous solutions (with and without salt addition) (Figure 1A). From pH 2.5 ($[HCl] = 10^{-2} M$), some aggregates appeared in the mixtures, characteristic of the formation of polyionic complexes (PICs). Aggregates were cohesive in the form of compact blocks (Figure 1A). PICs were still visible when the pH was increased up to 5.5. The addition of 400 mM NaCl weakened the PICs cohesion as blocks became granular suspensions (Figure 1A). Surprisingly, pure collagen solutions at pH 5.5 also exhibited a milky aspect with or without salt addition. (Figure 1B).

The analysis of collagen/THA solutions by cryo-scanning microscopy revealed sheet-like ultrastructure for the mixtures at pH 1, 2.5 and 4, regardless of the addition of NaCl. At pH 4.5 and 5.5, numerous fibrils appeared in the collagen/THA solutions (Figure 1A). Fibrils were also visible in pure collagen solutions at the same pHs, suggesting they were present before mixing. The thermal stability of collagen was analyzed within the mixtures by DSC. The collagen denaturation temperature was not significantly modified in the presence of THA but it was influenced by the presence of NaCl. At pH 1, the denaturation temperature was around 37°C which is similar to that of collagen in acetic acid (Figure 1C). From pH 2.5, the denaturation temperature of collagen in mixtures slightly increased to reach around 40 °C at pH 4. At this pH, the addition of 400 mM of NaCl dramatically increased the collagen denaturation temperature up to around 55 °C. The same phenomenon was observed for mixtures at pH 4.5 and 5.5 with salt (Figure 1C). Interestingly, the same denaturation temperature was measured for pure collagen solutions prepared with 400 mM NaCl from pH 4 to 5.5 (Figure 1C).

The observation of a homogenous solution at pH 1 shows that the PICs formation was inhibited in high acidic conditions as previously reported¹³. Carboxylic acid moieties on THA have a pKa around 2.5-3²². Hence, below this pH value, carboxylic acids are protonated,

resulting in a neutralization of the macromolecular chain. This neutrality drastically decreases the electrostatic attractions between collagen and hyaluronic acid, thereby preventing complexation. From pH 2.5 without salt, PICs appeared which could be attributed to a strong interaction between positively charged collagen and THA, negatively charged at this pH. The addition of NaCl screened the charges on biopolymer's chains and inhibits the PICs cohesion¹⁷. At pH 4, the addition of NaCl was not sufficient to prevent this complexation. However, NaCl might contribute to weaken PICs formation by increasing ionic strength in the macromolecular mixture and partially screened electrostatic attractions between biopolymers. For pH 4 and above in presence of salt, the temperature of denaturation increased up to 55 °C for pure collagen solutions and collagen/THA mixtures, which is the value for collagen fibrils. This suggests that collagen fibrillogenesis occurred in collagen solutions prior to mixing. Cryo-SEM confirms this hypothesis as fibrils were visible in pure collagen solutions and mixes at pH 4.5 and 5.5. The isoelectric point of collagen being around 6, the presence of fibrils in these solutions is justified^{23,24}. It was previously shown that the self-assembly of collagen into fibrils occurs at lower pH, however it leads to immature fibrils with an inferior stability and small size⁷. The self-assembly of collagen into fibrils also occurred at pH 4.5 and 5.5 without salt but the denaturation temperature was lower (around 45 °C). This indicates that the presence of salt allowed an appropriate fibrillogenesis and stabilized fibrils thanks to the adequate ionic strength. As the collagen fibril surface is quasi neutral, this could limit its interaction with THA⁷. Hence, the addition of salts prevents PIC's formation at very acid pH (2.5) due to charge screening and at high pH (from 4.5) thanks to the formation of collagen fibrils in solution.

Taguchi and collaborators have shown PICs formation can be inhibited in the presence of salt with 400mM NaCl as the optimal salt concentration to hinder electrostatic interactions

between collagen and THA at low pH values ¹³. Chen et al. extended this study by showing a shielding transitional area around 100 mM NaCl ¹⁷. In this transitional area, ionic strength is too low to screen interactions between both biopolymers but weakens it. Therefore, PIC formation depends on the balance between ionic strength and the strength of attractive interactions between collagen and THA.

3.2. Collagen gelling and fibrillogenesis within COL/THA hydrogels

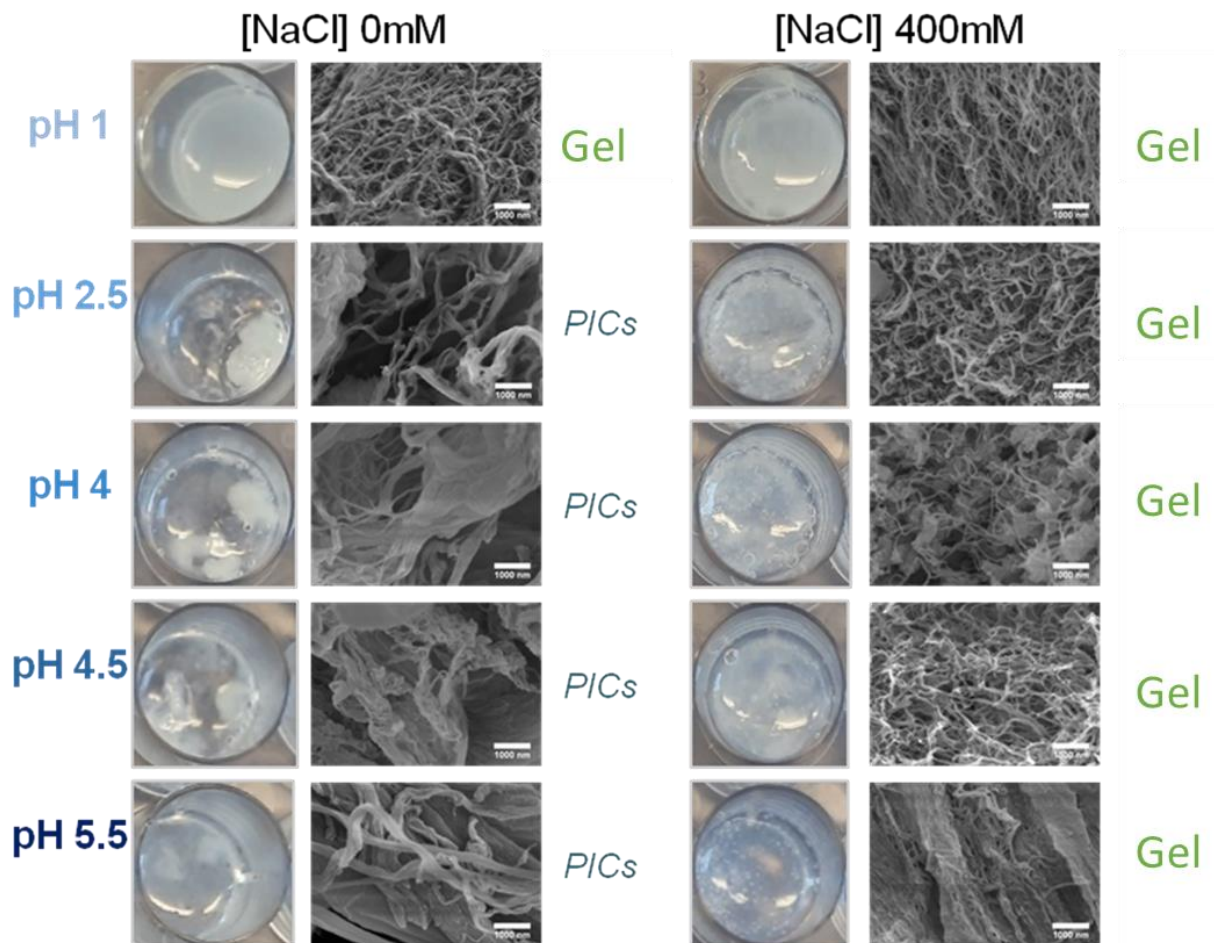


Figure 2 : Ultrastructure of Collagen/THA hydrogels observed after collagen gelling by scanning electron microscopy (scale bar: 1 μ m).

The ability of collagen/THA mixtures to gel and form collagen fibrils was investigated. For this purpose, collagen fibrillogenesis and gelling were triggered by neutralization. Hard gels were formed from collagen/THA solutions at pH 1 without or with salt (Figure 2). These gels exhibited a homogenous fibrillar network (Figure 2), thereby evidencing that collagen fibrillogenesis occurred properly. These hydrogels exhibited an ultrastructure similar to that of pure collagen hydrogels. For collagen/THA mixtures formed at pH 2.5 to 5.5 without salt addition, PICs were observed and hydrogels were not formed (Figure.2). PICs swelled during the ammonia exposure, but the aggregates were still visible. These materials were populated by thick fibrils or sheets, disorganized and massive (Figure.2). Despite PICs formation in solution, collagen fibrils could be formed, however their morphology seems to be disturbed by the presence of THA.

Chen et al previously observed this phenomenon by 2D IR mapping and reported a modification in the triple helical structure of collagen due to the presence of HA at low NaCl concentrations ¹⁷. However, the expected amide I band was visible by increasing the NaCl concentration, evidencing collagen α -helical structure was recovered. Hence, collagen was more prone to form fibrils. In this study, we confirm these results as individual fibrils are observed when 400 mM NaCl was added to collagen/THA mixtures. In addition, soft hydrogels were formed (Figure 2), suggesting that the PICs formation was limited enough to allow collagen gelling.

In more details, for initial solutions at pH 1 and pH 2.5 with salt addition, a homogenous fibrillar collagen network was visible similar to that observable in pure collagen hydrogels. For mixtures at pH 4, fibrillogenesis seemed to be disturbed as small aggregates were formed (Figure 2). Better defined collagen fibrils were observed in the pH 4.5 initial conditions while at pH 5.5, hydrogels were populated by well- defined collagen fibrils with a regular thickness.

Despite different structures, collagen has the same denaturation temperature around 52 °C in all gels, indicating that the thermal stability of fibrils was not altered by the ultrastructural modifications (Supporting Information 1).

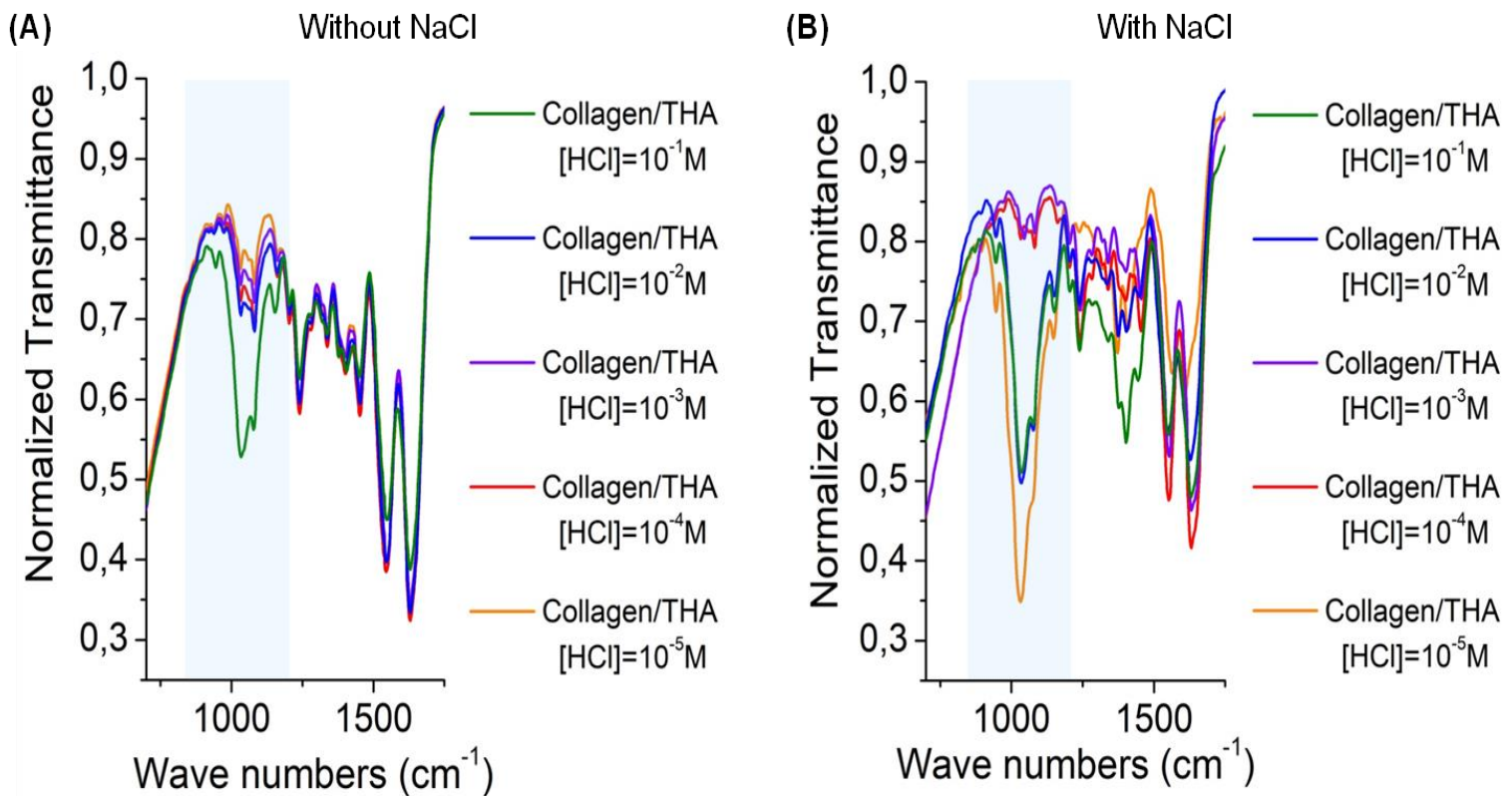


Figure 3: ATR-FTIR spectra of collagen/THA composite hydrogels after collagen gelling (A) without salt addition (B) and with 400 mM NaCl (zoom in the range from 750 to 1750 cm^{-1}).

The collagen/THA interactions within composite hydrogels were investigated by ATR-FTIR after collagen gelling. We specifically focused on the 750-1750 cm^{-1} wavenumber range that includes characteristic vibration bands of proteins (Amide I at 1650 cm^{-1} , Amide II at 1550 cm^{-1} , d(CH₃) and d(CH₂) between 1480 and 1350 cm^{-1} , Amide III between 1300 and 1200 cm^{-1}) (Supporting information 2). In this region, hyaluronan also exhibits several vibration bands at

1620 cm^{-1} and 1420 cm^{-1} corresponding to the carboxylate moieties (Supporting information 2). In the 900-1200 cm^{-1} range, two peaks at 1030 and 1080 cm^{-1} corresponding to d(C-O) and d(C-O-C) of carbohydrate moieties are observed for both polymers, but they are of high intensity in THA and of low intensity in acidic collagen (Supporting information 2). In the absence of salt, these peaks are observed in this range for composite hydrogels synthesized from solutions at pH 1 (Figure 3A). This is in good agreement with the fact that this is the only condition where the collagen gelling and fibrillogenesis occur without PICs formation (Figure 3A). In parallel, the similarity between all other spectra for solutions at higher pHs suggest that the formed PICs share a common chemical structure (Figure 3A and Electronic Supplementary Information N°3).

In contrast, in the presence of salts, spectra show important variations with initial pH (Figure 3B and Electronic Supplementary Information N°3). This would point out that, despite the fact that the final pH is the same for all conditions, the presence of the salt in the solutions leads to distinct chemical structures after gel formation. This should reflect that pH conditions have a strong influence on the protonation state of the charged moieties of both polymers but also on their conformation (Figure 3B). Similar to conditions without salts, the peaks at 1030-1080 cm^{-1} drastically decreased when the PICs were observed, suggesting the strong interaction with collagen modified the vibration of carbohydrate moieties. At pH 2.5 with NaCl addition, these peaks were visible, suggesting THA was in a free form (Electronic Supplementary Information N°3). This shows that PICs are no longer formed in these conditions and confirms that the addition of salt screens the charges to prevent the PICs formation¹⁷. At pH 4 and 4.5, the spectra resemble those obtained without salt addition when the PICs are present (Figure 3B). At pH 5.5, the peaks at 1030-1080 cm^{-1} were observed, suggesting collagen/THA

interactions are weak at a pH close to the collagen isoelectric point (Figure 3B and Electronic Supplementary Information N°3).

To summarize, well-fibrillated collagen networks were formed where PICS formation could be avoided, *i.e.* at low pH thanks to the screening of polymers charge and at high pH where collagen fibrillogenesis occurs before HA addition.

Usually, biomaterials synthesized from stable collagen/THA solution without the presence of PICS are sponges and not hydrogels¹⁷. Other studies have been carried to form homogeneous collagen/HA hydrogels but they do not take into account the complexation phenomenon^{15,25}. These systems were homogeneous due to the specific conditions. Actually, gelation was conducted at cold temperature with a pre-neutralization of collagen concomitant to the THA gelling by enzymatic crosslinking¹⁵. Cold temperature only slows down gelling of neutralized collagen. As a consequence, it is impossible to use this formulation to develop a homogenous ink for 3D printing or electrospinning as the gelling is not controllable or tunable.

3.3. THA gelling by enzymatic or photocrosslinking

Subsequently to the collagen gelation, THA crosslinking was performed to form the hyaluronan network. The efficacy of photocrosslinking (using eosin Y and green led light) was investigated and compared to enzymatic crosslinking using HRP/H₂O₂. The final goal was to create a double network and reinforce the collagen/THA hydrogel structure. The impact of THA crosslinking on the collagen network was studied through SEM observations (Figure 4). Only the conditions which allow the formation of homogenous hydrogels, *i.e.* in presence of 400 mM NaCl, are presented on Figure 4. The THA crosslinking did not impact the collagen/THA hydrogel ultrastructure as a homogeneous fibrillar network was observed

regardless of the HCl concentration considered. This ultrastructure resembled that of pure collagen hydrogels. Hence, the formation of di-tyramine bonds of the THA network does not modify the collagen ultrastructure. The porosity seems to be large enough and the interaction between both biopolymers small enough to generate an interpenetrating network.

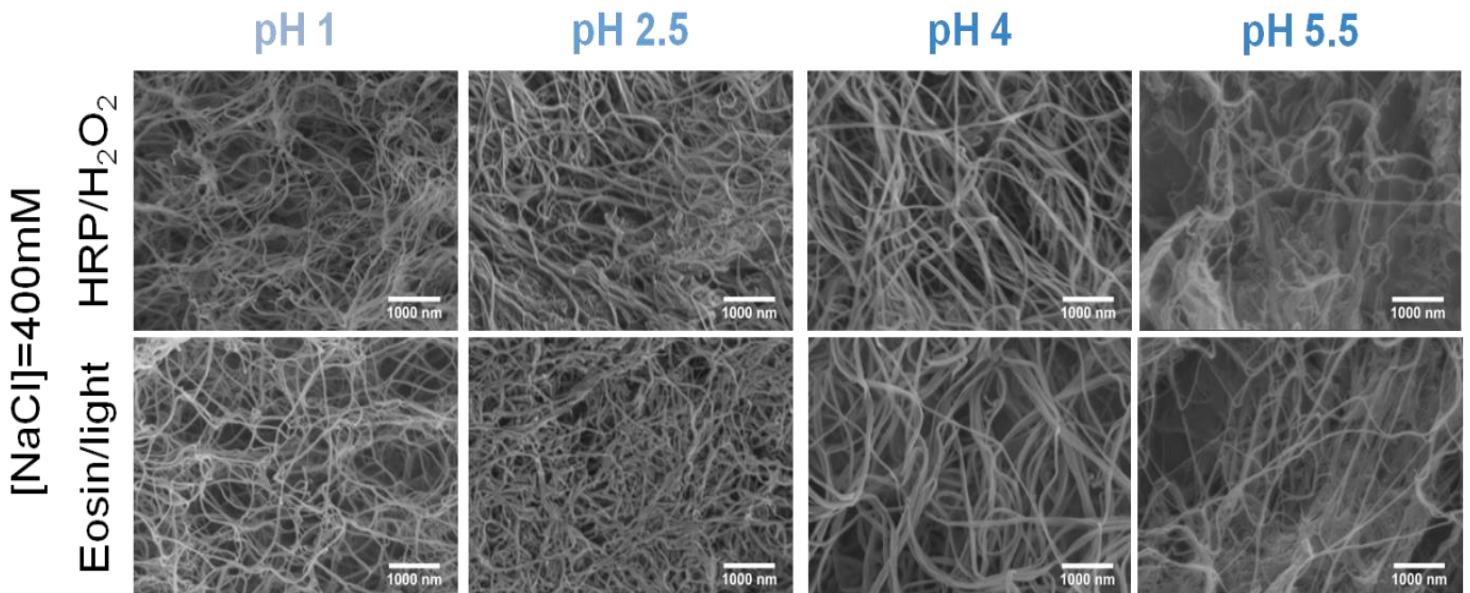


Figure 4: Ultrastructure of collagen/THA hydrogels from solutions with salt after enzymatic crosslinking or photocrosslinking (scale bar: 1 μ m).

The collagen thermal stability was investigated after THA crosslinking. The denaturation temperature was affected by the crosslinking method as shown in Figure 5A. Regarding the enzymatic crosslinking by HRP/H₂O₂, collagen in composite hydrogels underwent denaturation at around 53 °C, *i.e.* the same denaturation temperature found in pure collagen hydrogels. This suggests that the formation of the THA gel did not stabilize or destabilize collagen and no covalent bonds were formed between both polymers. In the composites photocrosslinked by green light, the collagen denaturation temperature increased up to 62 °C (Figure 5A). This increase means that photocrosslinking stabilized the collagen network and

reinforced it. Since collagen has tyrosine in its sequence ²⁶, amino acid similar to tyramine, a hybrid network could be formed using photocrosslinking. Besides the Tyramine/Tyramine bonds forming the THA network, a hybrid network could be generated by the formation of Tyramine/Tyrosine bonds. In addition, the collagen network could also be reinforced by the creation of Tyrosine/Tyrosine bonds between two collagen fibrils. Altogether, this could explain the higher denaturation temperature measured in photocrosslinked collagen/THA hydrogels. This hypothesis is supported by the increase in denaturation temperature up to 59°C in pure collagen hydrogel after photocrosslinking, indicating fibrils were stabilized possibly through new Tyrosine/Tyrosine covalent bonds ^{27,28}. The difference of collagen denaturation temperature between pure and Collagen/THA hydrogels could be due to the formation of supplementary Tyrosine/Tyramine bounds.

Rheological analysis revealed a decrease of storage modulus after enzymatic crosslinking in all conditions except for 10⁻⁵ M HCl (pH 5.5) (Figure 5B). Hence, HRP/H₂O₂ was inefficient to trigger THA network formation after collagen gelling and altered the hydrogel mechanical properties. The absence of THA network formation could be due to the weak diffusion of HRP within the fibrillated collagen network. Besides, the drop in mechanical properties may reflect partial depolymerization of THA induced by H₂O₂ ²⁹. The slight increase observed for 10⁻⁵ M HCl in the presence of salt could be attributed to the preformed fibrils in the solution. Consequently, fewer collagen molecules are available to form a gel, and the porosity could be higher. Then, the HRP diffusion could be facilitated.

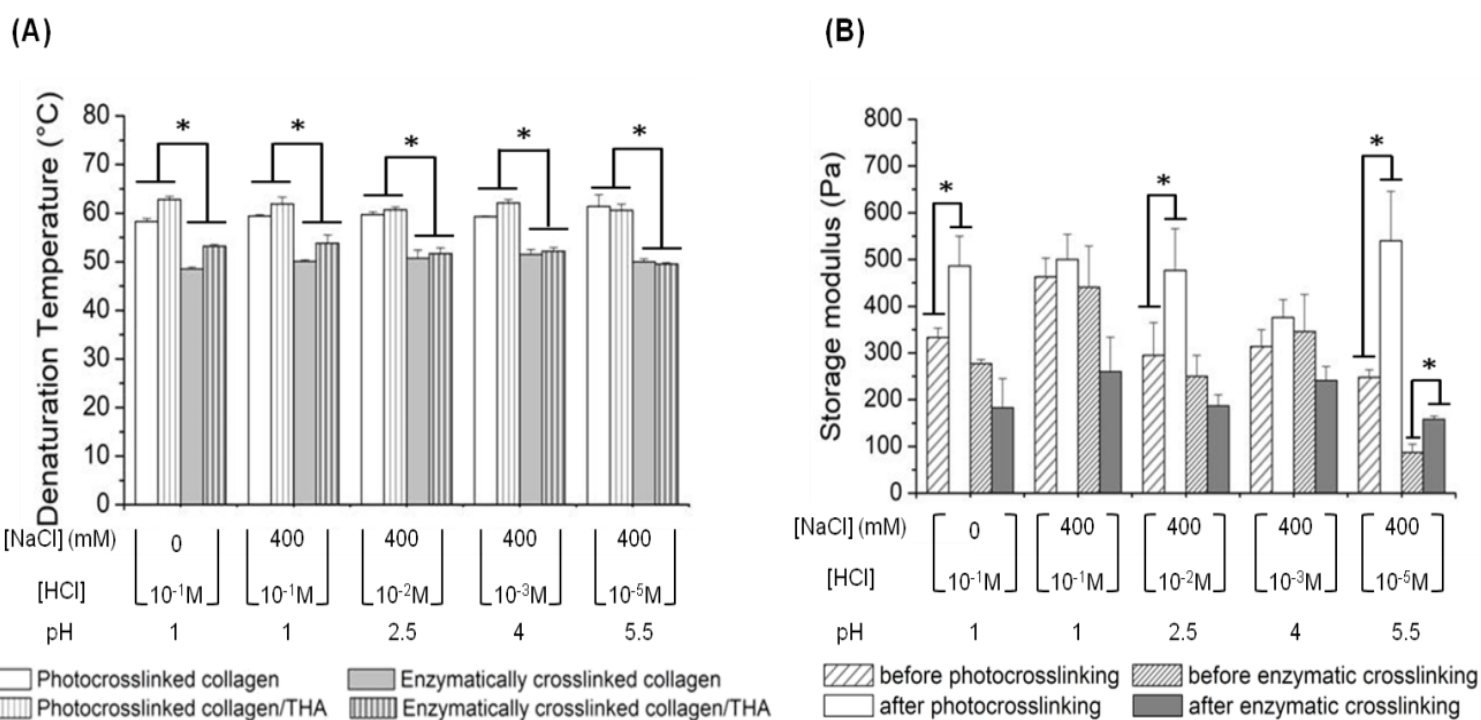


Figure 3 : (A) Collagen denaturation temperature of fibrillated hydrogels before and after THA crosslinking analyzed by DSC (B) Storage modulus of fibrillated hydrogels before and after THA crosslinking measured by rheometry. *: $p < 0.05$ ($n=3$).

Enzymatic crosslinking using HRP/H₂O₂ hydrogels has previously been investigated on collagen/THA²⁵. HRP was found effective in these systems because crosslinking was triggered during the co-gelation of pre-neutralized THA and collagen mixtures. In these conditions, no polyionic complexes were formed but the gelling was fast and not controllable after neutralization.

The storage modulus increased after photocrosslinking using Eosin Y and green light. Unlike HRP, eosin is a small molecule, thus it can easily diffuse within the collagen fibrillary network to the THA molecules. The condition for which the storage modulus gain was the highest were at pH 5.5 with salt (10^{-5} M HCl) as the storage modulus doubled. This is correlated to the

inhibition of PICs and the formation of homogenous gels. Since tyrosine amino acids are located at the fibril surface³⁰, covalent bonds could be formed between collagen fibrils or with THA, as previously mentioned. These crosslinkings would reinforce the polymeric structure and could explain the increase of mechanical properties. Therefore, photocrosslinking seems to be the optimal way to crosslink THA since it promotes the best structural, thermal and mechanical properties to the as-obtained hydrogel.

To fabricate composite hydrogels, several strategies have been tested. To obtain homogenous hydrogels, with suitable physical properties, polyionic complexation has to be inhibited somehow. The most developed materials rely on the use of EDC/NHS, photocrosslinking or enzymatic crosslinking of preneutralized collagen/HA solutions. This one pot technique seems to be the most promising method to target a wide range in swelling and mechanical properties³¹⁻³⁴. However, fibrillogenesis is inhibited, thus the physiological topography cannot be reproduced. In addition, the high crosslinking between polymers inhibit biological degradation and water retention¹⁵. Last, long term procedures cannot be performed as collagen gelling rapidly occurs. Hence, our novel procedure to produce collagen/THA hydrogels seems to be promising for biomedical applications.

4. Conclusion

This study describes an original method to inhibit the polyionic complexation between collagen and hyaluronic acid-tyramine, thereby generating homogenous and biomimetic composite hydrogels. Unlike the common strategy based on the utilization of highly acidic solutions (pH 1), it is possible to form composite hydrogels using solutions with a pH close to the collagen isoelectric point (pH 5.5). In this condition, stable and mature collagen fibrils are

generated in solution, which can homogeneously be mixed with hyaluronic acid without triggering any polyionic complexation. Subsequently, collagen gelling can be performed by pH increase. The method presented is compatible with a secondary crosslinking mechanism by forming di-tyramine bonds using eosin and green light to modulate composite hydrogels' physical and rheological properties without altering their structure. Taken together, these results show collagen and THA can be mixed at pH near physiological conditions, *i.e.* compatible with cells survival, then used to synthesize biomaterials for tissue engineering applications.

Acknowledgements

This project has been supported by "L'Agence Nationale de la Recherche" (ANR) and the Swiss National Science Foundation (SNSF): INDEED project, SNSF's grant number 310030E_189310 and ANR's grant number ANR-19-CE06-0028. We thank Dr. Francisco Fernandes for his helpful advices.

Supporting Information

Supporting Information is available from XX.

Declaration of competing interests

The authors declare no conflict of interests relevant to this work.

References

- 1 S. Ullah and X. Chen, *Applied Materials Today*, 2020, **20**, 100656.
- 2 M. Khanmohammadi, M. B. Dastjerdi, A. Ai, A. Ahmadi, A. Godarzi, A. Rahimi and J. Ai, *Biomater. Sci.*, 2018, **6**, 1286–1298.
- 3 H. Chamkouri, *AJBSR*, 2021, **11**, 485–493.
- 4 T. Biswal, *Materials Today: Proceedings*, 2021, **41**, 397–402.
- 5 S. Van Vlierberghe, P. Dubruel and E. Schacht, *Biomacromolecules*, 2011, **12**, 1387–1408.
- 6 K. E. Kadler, C. Baldock, J. Bella and R. P. Boot-Handford, *Journal of Cell Science*, 2007, **120**, 1955–1958.
- 7 F. Gobeaux, G. Mosser, A. Anglo, P. Panine, P. Davidson, M.-M. Giraud-Guille and E. Belamie, *Journal of Molecular Biology*, 2008, **376**, 1509–1522.
- 8 J. A. Burdick and G. D. Prestwich, *Adv. Mater.*, 2011, **23**, H41–H56.
- 9 R. Wang, X. Huang, B. Zoetebier, P. J. Dijkstra and M. Karperien, *Bioactive Materials*, 2023, **20**, 53–63.
- 10 D. Petta, D. W. Grijpma, M. Alini, D. Eglin and M. D’Este, *ACS Biomater. Sci. Eng.*, 2018, **4**, 3088–3098.
- 11 A. Zennifer, S. Manivannan, S. Sethuraman, S. G. Kumbar and D. Sundaramurthi, *Biomaterials Advances*, 2022, **134**, 112576.
- 12 C. Loebel, S. E. Szczesny, B. D. Cosgrove, M. Alini, M. Zenobi-Wong, R. L. Mauck and D. Eglin, *Biomacromolecules*, 2017, **18**, 855–864.
- 13 T. Taguchi, T. Ikoma and J. Tanaka, *J. Biomed. Mater. Res.*, 2002, **61**, 330–336.
- 14 Q. Xu, J. E. Torres, M. Hakim, P. M. Babiak, P. Pal, C. M. Battistoni, M. Nguyen, A. Panitch, L. Solorio and J. C. Liu, *Materials Science and Engineering: R: Reports*, 2021, **146**, 100641.
- 15 A. Frayssinet, D. Petta, C. Illoul, B. Haye, A. Markitantova, D. Eglin, G. Mosser, M. D’Este and C. H elary, *Carbohydrate Polymers*, 2020, **236**, 116042.
- 16 S. T. Kreger and S. L. Voytik-Harbin, *Matrix Biology*, 2009, **28**, 336–346.
- 17 S. Chen, Q. Zhang, T. Nakamoto, N. Kawazoe and G. Chen, *J. Mater. Chem. B*, 2014, **2**, 5612–5619.
- 18 E.  yszczarz, W. Brniak, J. Szafraniec-Szczesny, T. M. Majka, D. Majda, M. Zych, K. Pielichowski and R. Jachowicz, *Pharmaceutics*, 2021, **13**, 1122.
- 19 M. Camman, P. Joanne, J. Brun, A. Marcellan, J. Dumont, O. Agbulut and C. H elary, *Biomaterials Advances*, 2023, **144**, 213219.
- 20 Imanuel. Bergman and Roy. Loxley, *Anal. Chem.*, 1963, **35**, 1961–1965.
- 21 C. Loebel, M. D’Este, M. Alini, M. Zenobi-Wong and D. Eglin, *Carbohydrate Polymers*, 2015, **115**, 325–333.
- 22 M. Brown and S. Jones, *J Eur Acad Dermatol Venerol*, 2005, **19**, 308–318.
- 23 J. M. Cassel and J. R. Kanagy, *J. RES. NATL. BUR. STAN.*, 1949, **42**, 557.
- 24 S.-H. Park, T. Song, T. S. Bae, G. Khang, B. H. Choi, S. R. Park and B.-H. Min, *Int. J. Precis. Eng. Manuf.*, 2012, **13**, 2059–2066.
- 25 A. Schwab, C. H elary, R. G. Richards, M. Alini, D. Eglin and M. D’Este, *Materials Today Bio*, 2020, **7**, 100058.
- 26 J. H. Bowes and R. H. Kenten, *Biochemical Journal*, 1948, **43**, 358–365.
- 27 M. E. Carnes, C. R. Gonyea, R. G. Mooney, J. W. Njihia, J. M. Coburn and G. D. Pins, *Tissue Engineering Part C: Methods*, 2020, **26**, 317–331.
- 28 X. Zhang, S. Xu, L. Shen and G. Li, *J Leather Sci Eng*, 2020, **2**, 19.
- 29 K. Yamazaki, K. Fukuda, M. Matsukawa, F. Hara, K. Yoshida, M. Akagi, H. Munakata and C. Hamanishi, *Pathophysiology*, 2003, **9**, 215–220.
- 30 M. Gauza-Włodarczyk, L. Kubisz and D. Włodarczyk, *International Journal of Biological Macromolecules*, 2017, **104**, 987–991.
- 31 L. Calderon, E. Collin, D. Velasco-Bayon, M. Murphy, D. O’Halloran and A. Pandit, *eCM*, 2010, **20**, 134–148.

- 33 H. Ying, J. Zhou, M. Wang, D. Su, Q. Ma, G. Lv and J. Chen, *Materials Science and Engineering: C*, 2019, **101**, 487–498.
- 34 T. Zhang, H. Chen, Y. Zhang, Y. Zan, T. Ni, M. Liu and R. Pei, *Colloids and Surfaces B: Biointerfaces*, 2019, **174**, 528–535.